

# Local adenoviral delivery of soluble CD200R-Ig enhances antitumor immunity by inhibiting CD200- $\beta$ -catenin-driven M2 macrophage

Seung-Phil Shin,<sup>1,5</sup> A-Ra Goh,<sup>1</sup> Ji-Min Ju,<sup>1</sup> Hyeon-Gu Kang,<sup>4</sup> Seok-Jun Kim,<sup>4</sup> Jong-Kwang Kim,<sup>2</sup> Eun-Jung Park,<sup>1</sup> Yong-Soo Bae,<sup>5</sup> Kyungho Choi,<sup>6,7,8</sup> Yuh-Seog Jung,<sup>1,3</sup> and Sang-Jin Lee<sup>1</sup>

<sup>1</sup>Division of Tumor Immunology, Research Institute & Hospital, National Cancer Center, Goyang, Gyeonggi-do 410-769, Republic of Korea; <sup>2</sup>Genome Analysis, Team Research Core Center, Research Institute & Hospital, National Cancer Center, Goyang, Republic of Korea; <sup>3</sup>Center for Thyroid Cancer, Department of Otorhinolaryngology, Research Institute & Hospital, National Cancer Center, Goyang, Republic of Korea; <sup>4</sup>Department of Biomedical Science, BK21-Plus Research Team for Bioactive Control Technology, College of Natural Sciences, Chosun University, 309 Pilmun-daero, Dong-gu, Gwangju 61452, Republic of Korea; <sup>5</sup>Department of Biological Sciences, SRC Center for Immune Research on Non-lymphoid Organs, Sungkyunkwan University, Jangan-gu, Suwon, Republic of Korea; <sup>6</sup>Department of Biochemistry and Molecular Biology, Seoul National University College of Medicine, Seoul, Republic of Korea; <sup>7</sup>Department of Biomedical Sciences, Seoul National University College of Medicine, Seoul, Republic of Korea; <sup>8</sup>Cancer Research Institute, Seoul National University College of Medicine, Seoul, Republic of Korea

**CD200 is known as an immune checkpoint molecule that inhibits innate immune cell activation. Using a head and neck squamous cell carcinoma (HNSCC) model, we sought to determine whether localized delivery of adenovirus-expressing sCD200R1-Ig, the soluble extracellular domain of CD200R1, enhances antitumor immunity. Mouse-derived bone marrow cells and M1/M2-like macrophages were cocultured with tumor cells and analyzed for macrophage polarization. As an *in vivo* model, C57BL/6 mice were subcutaneously injected with MEER/CD200<sup>High</sup> cells, CD200-overexpressing mouse HNSCC cells. Adenovirus-expressing sCD200R1-Ig (Ad5sCD200R1) was designed, and its effect was tested. Components in the tumor-immune microenvironment (TIME) were quantified using flow cytometry. CD200 promoted tumor growth and induced the expression of immune-related genes, especially macrophage colony-stimulating factor (M-CSF). Interestingly, CD200 induced M2-like polarization both *in vitro* and *in vivo*. Consequently, CD200 recruited more regulatory T (Treg) cells and fewer CD8<sup>+</sup> effector T cells. These effects were effectively abolished by local injection of Ad5sCD200R1. These protumor effects of CD200 were driven through the  $\beta$ -catenin/NF- $\kappa$ B/M-CSF axis. CD200 upregulated PD-L1, and the combined targeting of CD200 and PD-1 thus showed synergy. The immune checkpoint CD200 upregulated immune-related genes through  $\beta$ -catenin signaling, reprogrammed the TIME, and exerted protumor effects. Ad5sCD200R1 injection could be an effective targeted strategy to enhance antitumor immunoeediting.**

## INTRODUCTION

Immune checkpoint inhibitors such as anti-PD-1 and anti-CTLA4 antibodies opened a new era of antitumor immunotherapy by showing notable clinical benefits in the treatment of solid cancers.<sup>1–4</sup> Most current immune checkpoint inhibitors, including those directed against

more recent targets such as LAG3 and TIGIT, aim to enhance anti-tumor T cell activation rather than innate immune cell activation. Among these molecules, CD200 is known as an immune checkpoint molecule that inhibits innate immune cell activation. CD200 is expressed on the surface of various tumor cell types.<sup>5,6</sup> Its receptor, CD200R1, is mostly expressed on myeloid cells, including macrophages.<sup>7,8</sup> The CD200-CD200R1 interaction delivers an inhibitory signal to myeloid cells, leading to their inactivation,<sup>9</sup> and also regulates myeloid-derived suppressor cell (MDSC) expansion in the pancreatic ductal adenocarcinoma (PDAC), creating immune-suppressive microenvironment.<sup>10</sup> Therefore, CD200 represents an innate arm of immune checkpoints that tumor cells utilize for immune evasion, and it has been suggested as a promising immunotherapeutic target. Accordingly, CD200-blocking strategies, including anti-CD200 antibodies, have been reported by several groups.<sup>10,11</sup>

Although antibody-based immune checkpoint inhibitors attract attention, their systemic use is always accompanied by a certain degree of autoimmunity via enhancement of general systemic immune responses. Anti-CTLA4 antibody therapy shows the most evident autoimmune side effects. Anti-PD-1 antibody therapy is also accompanied by some degree of autoimmunity, although the effect

Received 15 May 2021; accepted 8 September 2021;  
<https://doi.org/10.1016/j.omto.2021.09.001>.

**Correspondence:** Sang-Jin Lee, Division of Tumor Immunology, Research Institute & Hospital, National Cancer Center, Goyang, Gyeonggi-do 410-769, Republic of Korea.

**E-mail:** leesj@ncc.re.kr

**Correspondence:** Yuh-Seog Jung, Division of Tumor Immunology, Research Institute & Hospital, National Cancer Center, Goyang, Gyeonggi-do 410-769, Republic of Korea.

**E-mail:** jysorl@ncc.re.kr

**Correspondence:** Kyungho Choi, Cancer Research Institute, Seoul National University College of Medicine, Seoul, Republic of Korea.

**E-mail:** khchoi@snu.ac.kr

is milder than that of anti-CTLA4 therapy. Thus, localized delivery of immune checkpoint inhibitors is an alternative strategy to enhance antitumor immunity with minimal autoimmune side effects. We previously reported that local treatment with PD1-Ig-expressing adenovirus could augment antitumor immunity by strengthening CD8<sup>+</sup> T cell reactivity.<sup>12</sup> In accordance, localized delivery of CD200-blocking moieties such as soluble CD200R1-Ig (sCD200R1-Ig) may enhance antitumor immunity by targeting myeloid cells rather than T cells.

On the other hand, CD200 itself is known to deliver a protumoral intracellular signal in tumor cells. For example, we previously showed that CD200 induced epithelial-mesenchymal transition (EMT) in head and neck squamous cell carcinoma (HNSCC) cells.<sup>13</sup> However, it is not well known whether this inward CD200 signal in tumor cells grants tumor cells immunosuppressive properties. To study the immunomodulatory role of CD200 in tumor cells and to evaluate the effect of localized sCD200R1-Ig delivery, we adopted a syngeneic mouse tumor model of HNSCC.

In this study, we elucidated that CD200 stimulates the  $\beta$ -catenin/NF- $\kappa$ B/macrophage colony-stimulating factor (M-CSF) axis in tumor cells, which promotes M2 macrophage differentiation in the tumor immune microenvironment (TIME). Local inhibition of CD200 signaling by treatment with sCD200R1-Ig-expressing adenovirus effectively abolished the activity of this pathway, induced a switch from M2 to M1 polarization in macrophages, and showed profound therapeutic efficacy. Furthermore, we found that CD200 upregulates PD-L1 expression on tumor cells and that combined treatment with sCD200R1-Ig adenovirus and anti-PD1 antibody further potentiated the antitumor effect. Thus, inhibiting both checkpoint molecules suppressing T cells and myeloid cells by localized adenovirus delivery is a promising strategy to maximize antitumor immunity.

## RESULTS

### CD200 expression promotes HNSCC tumorigenesis

The Cancer Genome Atlas (TCGA) database analysis of HNSCC patients showed that the expression level of CD200 was closely associated with the degree of histological progression of tumors,<sup>13</sup> and CD200-overexpressing murine HNSCC cells were tumorigenic *in vivo*.<sup>13</sup> Hence, we hypothesized that CD200 on cancer cells may contribute to tumor initiation and progression and attempted to investigate whether CD200 can change the TIME by driving cytoplasmic intracellular signaling. We stably transfected MEER cells, murine HNSCC cells from C57/BL6 mice, with a CD200-expression plasmid and selected a clone (MEER/CD200<sup>High</sup>) that expressed a high level of CD200<sup>12</sup> (Figure S1A) but did not show any difference in proliferation *in vitro* compared to that of the control cell line (MEER/control) (Figure S1B). In contrast to this normal growth rate *in vitro*, MEER/control cells inoculated into syngeneic B6 mice did not show significant growth *in vivo*. In contrast, MEER/CD200<sup>High</sup> cells grew exponentially (Figure S1C). These results imply that CD200 on tumor cells may generate a tumor microenvironment favorable for tumor growth *in vivo*.

### Inhibition of tumor growth by CD200 neutralization

To confirm that the rapid tumor growth of MEER/CD200<sup>High</sup> cells is caused directly by CD200, we designed sCD200R1-Ig, the extracellular domain of the CD200 binding partner CD200R1 fused with the fragment crystallizable region (Fc) domain of mouse IgG2a, for neutralization of CD200. For delivery of sCD200R1-Ig to MEER/CD200<sup>High</sup> cells, a replication-deficient adenovirus harboring the sCD200R1-Ig gene under the control of the EF1 $\alpha$  promoter (Ad5sCD200R1) was constructed (Figure 1A). We assumed that MEER/CD200<sup>High</sup> cells transduced with Ad5sCD200R1 would generate and secrete sCD200R1-Ig proteins and that the secreted sCD200R1-Ig might bind to MEER/CD200<sup>High</sup> cells in an autocrine or paracrine manner to block CD200.

As expected, sCD200R1-Ig proteins were detected in lysates and culture supernatants of MEER/CD200<sup>High</sup> cells transduced with Ad5sCD200R1 (MOI, 10 or 100), whereas these proteins were not detected in cells transduced with empty adenovirus (Ad5MOCK) (Figure 1B). The specific binding activity of the secreted sCD200R1-Ig proteins was confirmed by detection of cell-bound sCD200R1-Ig on MEER/CD200<sup>High</sup> cells but not on MEER/control cells after treatment of those cells with the culture supernatant of the transduced cells (Figure 1C). Next, to evaluate whether the binding of sCD200R1 to CD200 can lead to tumor growth suppression, MEER/CD200<sup>High</sup> tumors were subcutaneously established and injected with Ad5sCD200R1. Ad5sCD200R1 effectively inhibited tumor growth, as shown in the left panel of Figure 1D. This growth inhibition was already evident within several days after the first virus injection, indicating the rapidity of the effect (Figure 1D, right panel). These data imply that the CD200-CD200R1 axis could be a potential target for suppressing the growth of CD200-expressing HNSCC tumors.

### Abundance of M2-like macrophages in CD200-overexpressing tumors

Although several published reports have noted that CD200 expression on tumor cells enhances tumor growth, the underlying mechanisms are largely unknown except for the assumption that CD200 engages CD200R1 on myeloid cells to inhibit their activation.<sup>11,14,15</sup> Furthermore, it is also unclear whether this inward CD200 signal in tumor cells endows these cells with their immunomodulatory capacity. Thus, we tried to identify tumor-intrinsic immunomodulatory factors in CD200-expressing HNSCC cells. For this purpose, the overexpressed genes in MEER/CD200<sup>High</sup> cells were investigated by RNA sequencing (RNA-seq). The transcript fold changes (criteria:  $p < 0.05$ , fold change  $> 1.5$ , normalized read count (RC) ( $\log_2$ )  $> 4$ ) between MEER/CD200<sup>High</sup> and MEER/control cells were analyzed in the gene set of the “immune response” category.<sup>16</sup> HNSCC tumors expressing CD200 in TCGA database were selected and explored with the RNA-seq data for the “immune response” category gene set in CD200-expressing HNSCC cells. This analysis showed that MEER/CD200<sup>High</sup> cells shared 322 genes with the human CD200<sup>+</sup> HNSCC group (Figure 2A, top panel) and that 12 genes were related to the immune response (Figure 2A, bottom panels). Interestingly, among those 12 genes was *CSF1*, also called M-CSF. The increased expression of M-CSF in MEER/CD200<sup>High</sup> cells compared with MEER/control

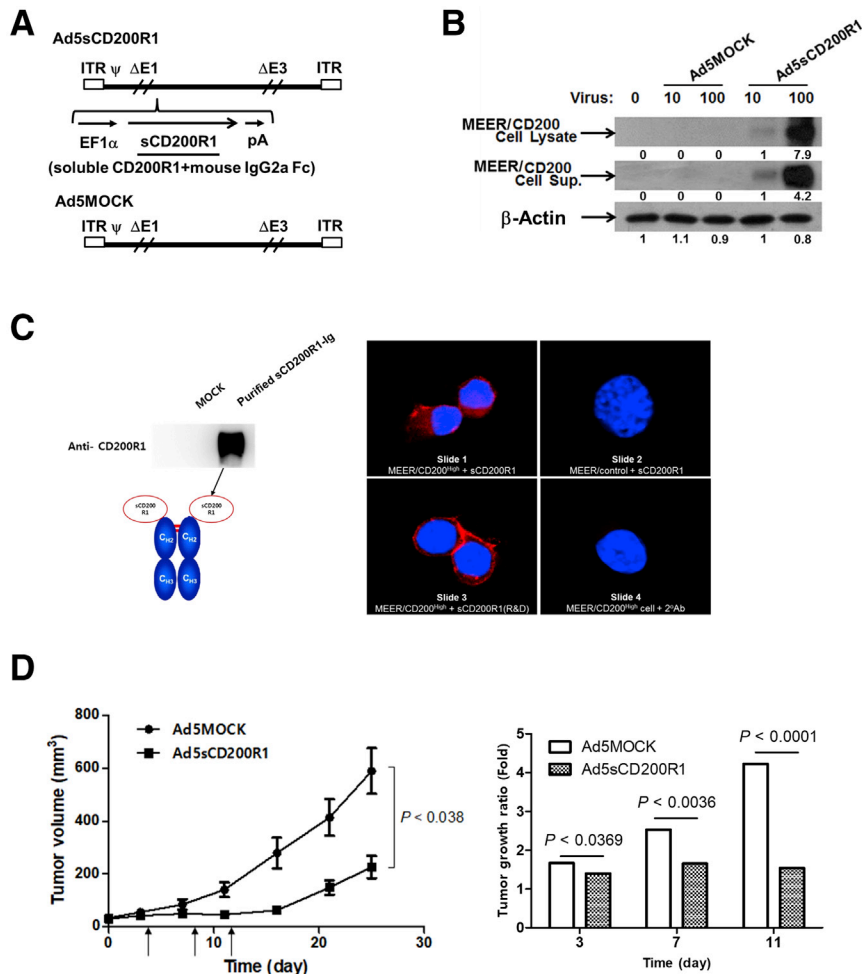


**Figure 1. Inhibition of tumor growth by CD200 blockade**

(A) A gene fused with the extracellular domain of CD200R1 and the Fc domain of mouse IgG2a was cloned into an adenoviral vector under the control of the EF1 $\alpha$  promoter to construct Ad5sCD200R1. Ad5MOCK adenovirus was constructed as a control. (B) MEER/CD200<sup>High</sup> cells were infected at MOIs of 10 and 100 for 2 h to confirm the secretion of soluble sCD200R1-Ig (sCD200R1-Ig) into the culture medium. Culture supernatant (Cell Sup.) was collected, and cells were lysed with RIPA buffer (Cell Lysate). Total protein (30  $\mu$ g) was separated for western blot analysis. (C) MEER/CD200<sup>High</sup> and MEER/control cells were immunostained with sCD200R1-Ig and with a rhodamine-conjugated anti-CD200R1 antibody. Cells were also stained with DAPI (4',6-diamidino-2-phenylindole). The binding of sCD200R1/CD200 was monitored by confocal microscopy. (D) (Left panel) C57BL/6 mice were inoculated subcutaneously in the flanks with MEER/CD200<sup>High</sup> cells ( $1 \times 10^6$ ) followed by intratumoral injection of  $5 \times 10^8$  plaque-forming units of either Ad5MOCK (filled circles) or Ad5sCD200R1 (filled squares) 3 times at 4-day intervals. Arrows indicate the times of adenovirus injection. (Right panel) Tumor growth rates are plotted with respect to the time of adenovirus treatment in the left panel. Ad5MOCK (empty bar) or Ad5sCD200R1 (checked bar). The data are presented as the mean  $\pm$  SEM values (n = 5).

cells was also confirmed at the protein level (Figure 2B). M-CSF is a cytokine involved in monocyte/macrophage differentiation and, more importantly, contributes to tumor-promoting M2 polarization of macrophages in the tumor microenvironment.<sup>17,18</sup> Thus, it is conceivable that in addition to the outward effects of CD200 on CD200R1 on macrophages, inward CD200 signaling in tumor cells grants them the capacity for macrophage skewing toward a more protumor phenotype. M-CSF may be one of the readouts of this macrophage-skewing capacity of CD200-expressing tumor cells. To evaluate this possibility *in vivo*, the F4/80<sup>+</sup>CD206<sup>-</sup> (M1-like)/F4/80<sup>+</sup>CD206<sup>+</sup> (M2-like) macrophage polarization ratio in tumor-infiltrating macrophages was analyzed in MEER/CD200<sup>High</sup> tumor-bearing mice. As the tumors grew, the macrophage phenotype underwent a significant shift toward an M2-like phenotype, supporting our hypothesis (Figure 2C).

#### Increased M2-like macrophages in the presence of MEER/CD200<sup>High</sup> cells *in vitro*

To test the M2-skewing capacity of CD200-expressing tumors more directly, we cocultured undifferentiated bone marrow cells (BMCs)

with MEER/CD200<sup>High</sup> cells and examined whether MEER/CD200<sup>High</sup> cells affect macrophage polarization during *in vitro* macrophage differentiation. First, the macrophage differentiation potential of BMCs was verified by cytokine-induced differentiation and polarization assays. BMCs were successfully differentiated into M1-like macrophages (F4/80<sup>+</sup>CD200R1<sup>+</sup>CD206<sup>-</sup>) by GM-CSF + interferon (IFN)- $\gamma$  or into M2-like macrophages (F4/80<sup>+</sup>CD200R1<sup>+</sup>CD206<sup>+</sup>) by M-CSF + interleukin (IL)-4. The polarity of the resulting macrophages was further confirmed by assessment of nitric oxide production (Figures S2A and S2B). Thus, these BMCs were fully capable of differentiation into macrophage-lineage cells. Then, when these BMCs were cocultured with MEER/CD200<sup>High</sup> cells *in vitro*, MEER/CD200<sup>High</sup> cells (M1/M2: 7.2) more dramatically induced M2 polarization than did MEER/control cells (M1/M2: 25.2) (Figure 3A). To further evaluate the M2-polarizing potential of MEER/CD200<sup>High</sup> cells, tumor cells were cocultured with pre-differentiated M1-like macrophages. Even under these conditions, MEER/CD200<sup>High</sup> cells (M1/M2: 11.1) induced M2 polarization relative to MEER/control cells (M1/M2: 25.1) (Figure 3B). However, there was no change in MEER/control (M1/M2: 0.44) and MEER/CD200<sup>High</sup> cells (M1/M2: 0.45) when we used predifferentiated M2-like macrophages (Figure 3C). Thus, MEER/CD200<sup>High</sup> cells acquired M2-polarizing capacity via expression of CD200 *in vivo* and *in vitro*.

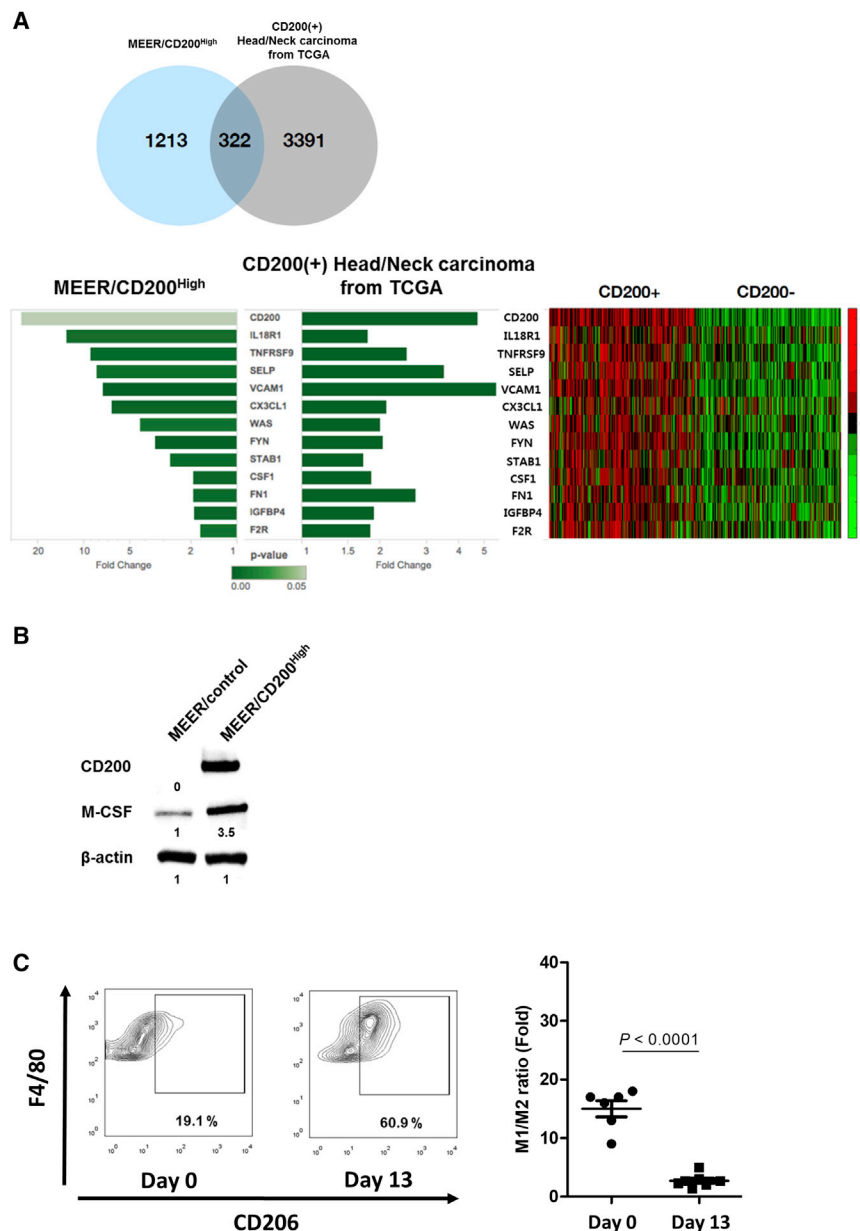


**Figure 2. M2-like macrophage differentiation in the CD200-overexpressing HNSCC tumor model**

(A) TCGA mRNA data for CD200-overexpressing HNSCC patients (n = 522) were compared using the fold change values of immune/inflammatory response genes in MEER/control and MEER/CD200<sup>High</sup> cells. A p value < 0.05 and a fold change > 1.5 were considered to indicate statistically significant differences in expression. (B) Total protein from MEER cell lines was extracted using RIPA buffer containing a phosphatase inhibitor. Protein expression was analyzed by western blotting using antibodies specific for the indicated genes. (C) For *ex vivo* analysis of the macrophage spectrum, MEER/CD200<sup>High</sup> tumors were implanted in C57BL/6 mice. When the tumors were palpable (day 0), they were harvested on day 0 and day 13. The ratio of M1/M2-like macrophages was calculated from the percentages of F4/80<sup>+</sup>CD206<sup>+</sup> macrophages as determined by flow cytometry. The left panel shows a representative flow cytometric analysis plot. The right panel shows the M1/M2-like macrophage ratios from 6 mice.

tio in the Ad5sCD200R1-treated group than in the Ad5MOCK-treated group (Figure 4A). These results were consistent with the immunohistochemical staining of M1-like macrophages (F4/80<sup>+</sup>iNOS<sup>+</sup>) (Figure 4B).

Then, to verify the direct involvement of sCD200R1-Ig in the correction of M2 polarization, we evaluated the effect of sCD200R1-Ig treatment on macrophage differentiation and polarization mediated by MEER/CD200<sup>High</sup> cells *in vitro*. When sCD200R1-Ig, obtained via Ad5sCD200R1 transduction, was added to the *in vitro* culture systems used in the experiment described above (Figure 4), M2 polarization was partially reversed to M1 polarization by sCD200R1-Ig treatment in both BMCs and differentiated M1-like macrophages cultured with MEER/CD200<sup>High</sup> cells (Figure 4C, D). Of interest, even for pre-differentiated M2-like macrophages cocultured with MEER/CD200<sup>High</sup> cells, which

were not able to be further polarized toward an M2 phenotype due to their strong M2 polarization, sCD200R1-Ig slightly but statistically significantly reversed the polarization of M2-like macrophages to an M1-like phenotype (M1/M2: 0.44 to 0.54) (Figure 4E). Therefore, adenoviral delivery of sCD200R1-Ig efficiently inhibited M2 polarization mediated by CD200 on tumor cells and facilitated M1 polarization.

Finally, to confirm that the inhibition of tumor growth by CD200 neutralization is caused by enhanced reactivity of macrophages, we depleted macrophages using clodronate. The enhanced tumor-

**The therapeutic effect of Ad5sCD200R1 is mediated by M1 polarization enhancement**

Next, we evaluated whether the therapeutic effect of Ad5sCD200R1 is dependent on the blockade of M2 polarization of tumor macrophages by MEER/CD200<sup>High</sup> cells and the resulting facilitation of antitumoral M1 polarization of macrophages. Subcutaneously growing MEER/CD200<sup>High</sup> tumors were injected with Ad5sCD200R1 or Ad5-MOCK, and the M1/M2 ratio of tumor-infiltrating macrophages was assessed after 11 days. Ad5sCD200R1-treated tumors showed a significant reduction in the M2-like macrophage proportion compared to that in Ad5MOCK-treated tumors, resulting in a higher M1/M2 ra-

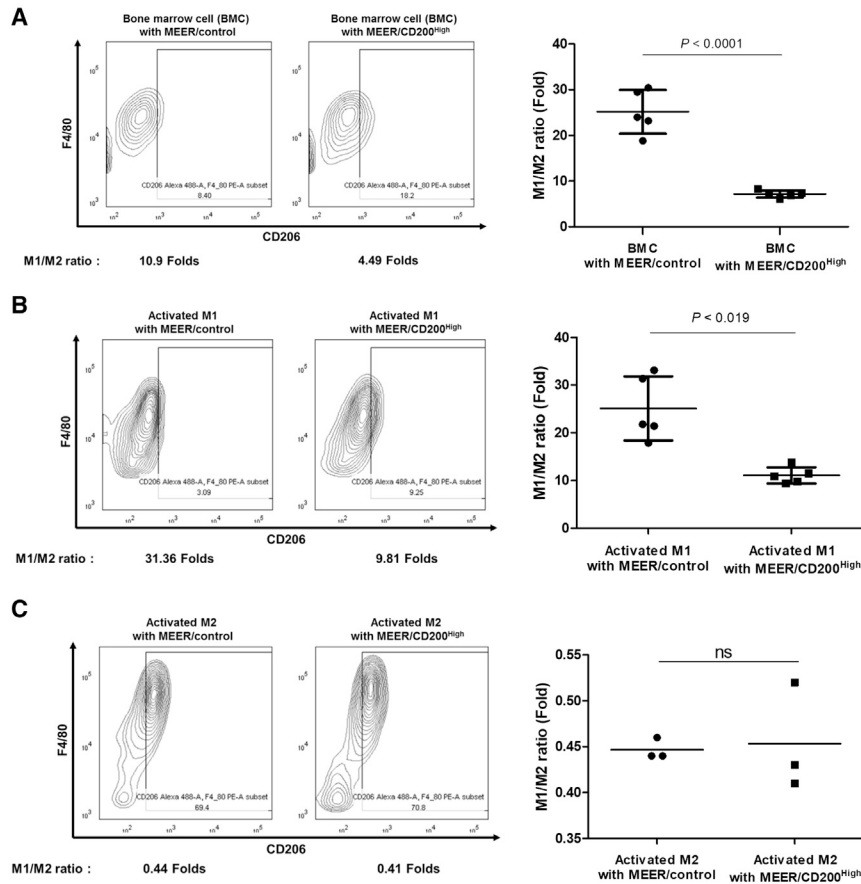


**Figure 3. Increase in polarization toward M2-like macrophages by overexpression of tumoral CD200**

(A) Bone marrow cells ( $2 \times 10^6$ ) from the tibias and femurs of C57BL/6 mice were cocultured with MEER/CD200<sup>High</sup> or MEER/control cells ( $2 \times 10^4$ ) for 5 days. When the tumors were palpable (day 0), they were harvested on day 0 and day 13. The ratio of M1/M2-like macrophages was calculated from the percentages of F4/80<sup>+</sup>CD206<sup>+</sup> macrophages as determined by flow cytometry. The right panel shows the M1/M2-like macrophage ratios from 5 mice. (B) Extracted bone marrow cells were treated with GM-CSF (10 ng/mL) and IFN- $\gamma$  (50 ng/mL) to induce differentiation into activated M1 macrophages and were then cocultured with MEER/control or MEER/CD200<sup>High</sup> cells for 3 days. The ratio of M1/M2-like macrophages was calculated as described in (B). (C) M2 macrophages activated by M-CSF (10 ng/mL) and IL-4 (10 ng/mL) were cocultured with MEER/control or MEER/CD200<sup>High</sup> cells for 3 days. The ratio of M1/M2-like macrophages was calculated as described in (B).

suppressive effect of Ad5sCD200R1 was almost completely abolished in macrophage-depleted mice (Figure 4F), further supporting the role of M1-skewed macrophages in this therapeutic setting.

#### Enhancement of M-CSF expression through the CD200/ $\beta$ -catenin interaction

We then explored the molecular mechanism by which CD200 on tumor cells can deliver intracellular signals leading to the acquisition of M2-polarizing capacity, as represented by enhanced M-CSF production, and tested whether sCD200R1-Ig could regulate this process. Since we observed that MEER/CD200<sup>High</sup> cells produced more M-CSF than MEER/control cells (Figure 2B), we further confirmed the influence of CD200 on M-CSF production by blocking CD200 in MEER/CD200<sup>High</sup> cells. First, Ad5sCD200R1-infected MEER/CD200<sup>High</sup> cells produced less M-CSF mRNA, probably via secretion of sCD200R1-Ig (Figure 5A). Consistent with this finding, CD200 siRNA (Figure 5B, left panel) or purified sCD200R1-Ig (Figure 5B, right panel) treatment reduced the M-CSF transcript abundance in MEER/CD200<sup>High</sup> cells. Next, we tried to identify a CD200 signaling pathway responsible for enhancing M-CSF transcription. It was reported that the cytoplasmic tail of CD200 is cleaved by  $\gamma$ -secretase and translocates to the nucleus.<sup>20</sup> We previously showed that the cleaved CD200 cytoplasmic tail interacts with  $\beta$ -catenin

and contributes to EMT in human HNSCC cells.<sup>12</sup> Therefore, we investigated whether the CD200- $\beta$ -catenin interaction also occurs in murine MEER/CD200<sup>High</sup> cells and is utilized for M-CSF production, which has not been studied before. We transfected MEER/control cells with the plasmid encoding the cytoplasmic tail (CD200/C-terminal) of CD200 fused with a 3 $\times$  FLAG tag and performed a coimmunoprecipitation assay, which confirmed the binding of the CD200 cytoplasmic tail to  $\beta$ -catenin (Figure 5C). This interaction was confirmed in both the cytosol and nucleus (Figure 5D). Moreover, the expression of the  $\beta$ -catenin target genes of c-MYC and S100A4 was increased (Figure 5E). Interestingly, the S100A4/RAGE signaling pathway is known to activate NF- $\kappa$ B,<sup>19</sup> which is reported to regulate M-CSF transcription.<sup>20</sup> Thus, we assessed the activation of the NF- $\kappa$ B pathway and found that CD200 overexpression resulted in a decrease in nuclear factor of kappa light polypeptide gene enhancer in B-cells inhibitor, alpha (I $\kappa$ B $\alpha$ ) phosphorylation and an increase in p65 and IKK phosphorylation in MEER/CD200<sup>High</sup> cells and subsequent enhancement of NF- $\kappa$ B transcriptional activity (Figures 5F and 5G). Consistent with this finding, NF- $\kappa$ B activation in MEER/CD200<sup>High</sup> cells was inhibited by treatment with CD200 siRNA and purified sCD200R1-Ig (Figures 5H and 5I). Inhibition of nuclear translocation of phosphorylated NF- $\kappa$ B by treatment with CD200 siRNA and Ad5sCD200R1 was also confirmed (Figure 5J). These data demonstrated that the interaction of the CD200 cytoplasmic tail with  $\beta$ -catenin may upregulate the production of the cytokine M-CSF through the NF- $\kappa$ B pathway, which is activated by the S100A4/RAGE pathway. Ad5sCD200R1 transduction and subsequent sCD200R1-Ig secretion can block this signaling to downregulate M-CSF production.

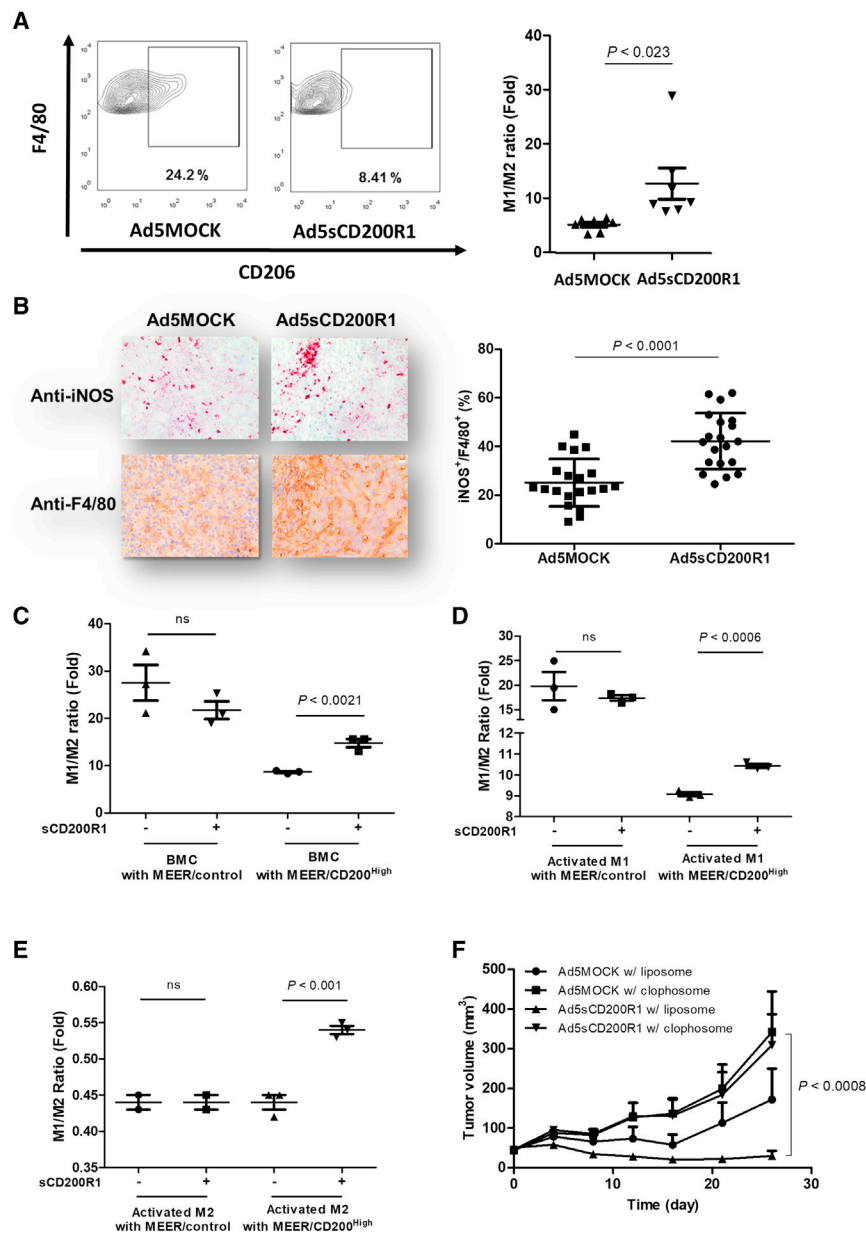


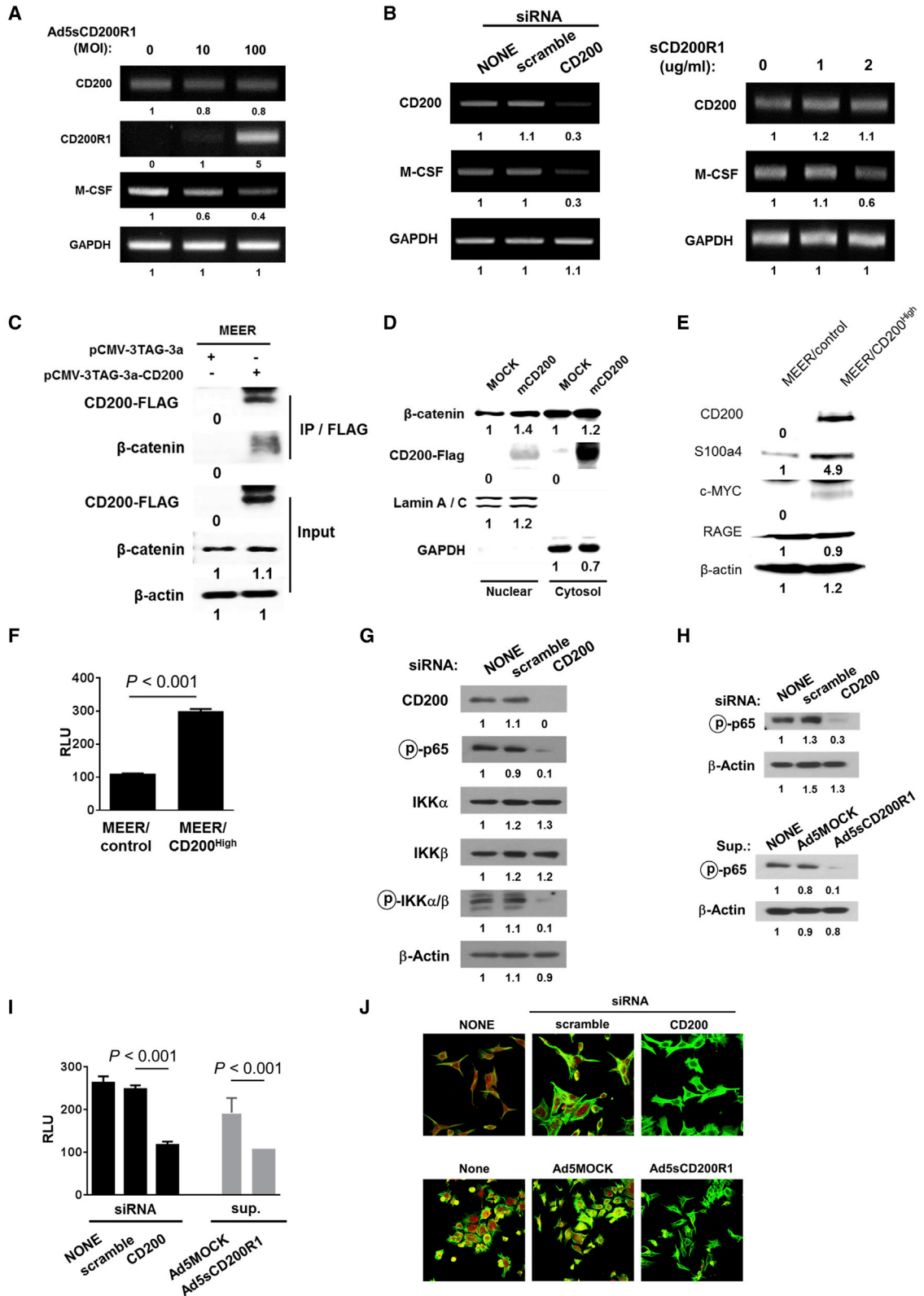
**Figure 4. M1-like macrophage differentiation and tumor regression induced by CD200R1-Ig**

(A) MEER/CD200<sup>High</sup> tumors in C57BL/6 mice were treated with adenovirus (day 7), Ad5MOCK (filled triangle), or Ad5sCD200R1 (inverted filled triangle). Two days after the second adenovirus injection, tumors were harvested and dissociated. The M1/M2-like macrophage ratio was calculated from the percentages of F4/80<sup>+</sup>CD206<sup>+</sup> macrophages as determined by flow cytometry. The left panel shows a representative flow cytometric analysis plot. The right panel shows the ratio of M1/M2-like macrophages from 7 mice. (B) C57BL/6 mice were subcutaneously injected with  $1 \times 10^6$  MEER/CD200<sup>High</sup> cells, and tumors were injected with  $5 \times 10^8$  PFUs of Ad5MOCK (filled square) and Ad5sCD200R1 (filled circle) 3 times at 4-day intervals when the volume reached approximately 60 mm<sup>3</sup>. The tumors were then harvested, and IHC was performed with the anti-F4/80 antibody, pan-macrophage marker, anti-iNOS antibody, and M1 marker. The cells in the stained tissues were directly counted and plotted (right panel). (C) MEER/control or MEER/CD200<sup>High</sup> cells were treated with 4  $\mu$ g of sCD200R1-Ig protein and cocultured with the extracted bone marrow cells for 3 days. The M1/M2 macrophage spectrum defined by the F4/80<sup>+</sup>/CD206<sup>+</sup> surface markers were analyzed by flow cytometry. (D) The extracted bone marrow cells were treated with GM-CSF (10 ng/mL) and IFN- $\gamma$  (50 ng/mL) to induce differentiation into activated M1 macrophages and were then cocultured with MEER/control or MEER/CD200<sup>High</sup> cells for 3 days. The M1/M2 macrophage spectrum was analyzed by flow cytometry as described in (C). (E) M2 macrophages activated by M-CSF (10 ng/mL) and IL-4 (10 ng/mL) were cocultured with MEER/control or MEER/CD200<sup>High</sup> cells for 3 days. The M1/M2 macrophage spectrum was analyzed by flow cytometry as described in (C). (F) Subcutaneous MEER/CD200<sup>High</sup> tumors in C57BL/6 mice were injected with  $5 \times 10^8$  PFUs of Ad5MOCK or Ad5sCD200R1. One day before virus treatment and every 4 days after treatment, mice were injected intraperitoneally with clodronate + liposomes or liposomes alone (first dose, 1.4 mg; subsequent doses, 0.7 mg) to deplete all macrophages. Tumor growth was calculated and plotted at the indicated time points. p values were determined by two-tailed paired t tests or by two-tailed unpaired t tests. M1, M1-like macrophage; M2, M2-like macrophage; BMC, bone marrow cell.

**T cell responses are necessary for the therapeutic effect of Ad5sCD200R1**

M1 polarization of macrophages in the tumor microenvironment not only potentiates the inflammatory properties of macrophages but also enhances T cell infiltration and activation.<sup>21</sup> Thus, M1 skewing by Ad5sCD200R1 treatment may alter tumor-infiltrating T cell responses. When we examined the tumor-infiltrating T cell population in MEER/CD200<sup>High</sup> tumor-bearing mice, Ad5sCD200R1-treated MEER/CD200<sup>High</sup> tumor tissue contained a very abundant T cell receptor (TCR)<sup>+</sup> cell population (Figure 6A) and a greater number of perforin<sup>+</sup>/IFN- $\gamma$ <sup>+</sup> effector CD8<sup>+</sup> T cells (Figure 6B) than the Ad5-

MOCK group. To evaluate whether this enhancement of T cell responses is necessary for the therapeutic efficacy of Ad5sCD200R1, we depleted CD8 T cells in the MEER/CD200<sup>High</sup> tumor model using an anti-CD8 depleting antibody. The inhibitory effect of Ad5sCD200R1 on tumor growth was nearly abolished by depletion of CD8<sup>+</sup> T cells (Figure 6C). Consistent with this finding, the anti-tumor effect of Ad5sCD200R1 was not observed in T cell-deficient nude mice inoculated with MEER/CD200<sup>High</sup> tumor cells (Figure 6D). In addition, the population of regulatory T (Treg) cells were monitored using C57BL/6-Tg (Foxp3-GFP)90Pkrj/J transgenic mice implanted with MEER/CD200<sup>High</sup> tumor (Figure 6E). Tumors treated



(legend on next page)

with  $5 \times 10^8$  PFUs of Ad5sCD200R1 included a smaller number of CD45<sup>+</sup>GFP<sup>+</sup> Treg cells and CD11b<sup>+</sup>CD206<sup>+</sup> M2 macrophages and, in contrast, exhibited increasing CD45<sup>+</sup>CD8<sup>+</sup> T cells. p values were determined by two-tailed unpaired t tests. Thus, T cell responses are critical for the therapeutic effect of local blockade of CD200, which indicates that targeting innate immune checkpoint molecules such as CD200 not only activates innate immune cells but also affects adaptive T cell responses and that this cooperation is required for full antitumor immunity.

#### Anti-tumor effects of dual blockade of PD1 and CD200

One way that the finding that CD200 blockade enhances T cell responses can be interpreted is that CD200 may potentiate the expression of T cell-inhibiting immune checkpoint molecules such as PD-L1. To test this hypothesis, we treated MEER/CD200<sup>High</sup> cells with IFN- $\gamma$  *in vitro* and examined PD-L1 expression. Surprisingly, PD-L1 expression was upregulated to a far greater extent in MEER/CD200<sup>High</sup> cells than in MEER/control cells (Figure 7A). Since MEER/control cells did not grow well *in vivo*, it was difficult to analyze PD-L1 expression on MEER/control cells *in vivo*. However, approximately 20% of MEER/CD200<sup>High</sup> cells expressed PD-L1 when grown subcutaneously (Figure S3), whereas *in-vitro*-cultured MEER/CD200<sup>High</sup> cells did not express PD-L1 (Figure 7A). Thus, CD200 may also affect PD-L1-mediated T cell inhibition.

Finally, to evaluate the potential synergistic effects of CD200- and PD-1-targeted combination therapies, Ad5sCD200R1 and anti-mouse PD1 antibody were co-administered in the MEER/CD200<sup>High</sup> mouse model. Tumor suppression was additively enhanced by this combination treatment of Ad5sCD200R1 and anti-mouse PD1 antibody (4/5 mice were tumor-free) compared with each monotherapy (Figures 7B and S4). Hence, local inhibition of innate checkpoint molecule by sCD200R1-Ig may be an attractive strategy for enhancing anti-PD1 immunotherapeutic efficacy.

## DISCUSSION

The immune checkpoint function of CD200 has been identified mainly in hematologic cancers such as acute myeloid leukemia (AML) but infrequently in solid cancers.<sup>8,22</sup> Additionally, CD200

stimulated the  $\beta$ -catenin/NF $\kappa$ B/M-CSF axis in tumor cells, leading to M2 macrophage polarization in the HNSCC model in this study, and it modulated cytokine signaling in MDSC in the PDAC model, resulting in MDSC expansion.<sup>10</sup> Inhibition of CD200 by local injection of adenovirus expressing sCD200R1-Ig effectively abolished the activity of this pathway, induced M1-like polarization, and thus had significant therapeutic efficacy. Furthermore, we showed a dramatic increase in PD-L1 expression in MEER/CD200<sup>High</sup> cells after IFN- $\gamma$  treatment *in vitro*. In line with the reported correlation in AML,<sup>8</sup> our data showed a similar pattern in a solid cancer, HNSCC. Considering that NF- $\kappa$ B and interferon regulatory factor (IRF) modulate PD-L1 expression, there could be shared signaling pathways linking PD-L1 and CD200. Accordingly, combined targeting of CD200 and PD-1 synergistically inhibited the growth of MEER/CD200<sup>High</sup> tumors. Combined targeting of these molecules by local injection of sCD200R1-Ig-expressing adenovirus and anti-PD1 antibody effectively inhibited the growth of MEER/CD200<sup>High</sup> tumors. This finding implies that antibodies inhibiting the PD-1/PD-L1 interaction would potentiate antitumoral effects with sCD200R1-Ig-expressing adenovirus.

HNSCC often occurs on mucosal surfaces of the larynx, throat, lips, mouth, nose, and salivary glands. The locoregional nature of HNSCC makes it accessible for both intratumoral injection and tissue biopsy. For this reason, it is one of the cancers in which adenovirus-based gene therapy is most frequently attempted. Here, the adenovirus Ad5sCD200R1, targeting CD200, was constructed to eventually attenuate tumor growth based on the observation that the adenovirus is the classical backbone for various gene therapies for HNSCC.<sup>23,24</sup> We observed that local injection of Ad5sCD200R1 effectively inhibited the growth of MEER/CD200<sup>High</sup> tumors and decreased M2-like macrophage polarization. This growth inhibition was abolished by macrophage depletion.

Beyond the previously shown nonimmunological function of CD200 in inducing EMT in HNSCC cells,<sup>13</sup> we initially sought to determine whether targeting CD200 affects tumor growth by modulating the TIME using the same model of HNSCC. Our mouse model exhibited increased M-CSF expression in CD200-overexpressing cells, similar to

#### Figure 5. M-CSF production in tumor cells by blocking CD200/ $\beta$ -catenin/NF $\kappa$ B signaling

(A) MEER/CD200<sup>High</sup> cells ( $1 \times 10^5$ ) were transduced with Ad5sCD200R1 at MOI of 10 or 100 for 2 h. Total RNA was extracted to evaluate the expression of each gene by RT-PCR as described in the materials and methods. (B) MEER/CD200<sup>High</sup> cells ( $1 \times 10^5$ ) were treated with 20 pmol of CD200 siRNA or scrambled siRNA for 24 h (left panel) and 1 or 2  $\mu$ g/ml sCD200R1-Ig purified from HEK293 cells transduced with Ad5sCD200R1 (right panel). Total RNA was extracted to evaluate the expression of each gene as described in (A). (C) Lysates of cells transfected with full-length CD200-3  $\times$  FLAG tag expression plasmids were precleared by incubation with protein-A/G linked agarose beads for 1 h. Precleared proteins were incubated with anti-FLAG M2 affinity gel overnight. Western blot analysis was then performed with anti-mouse  $\beta$ -catenin and anti-mouse CD200 antibodies. Data for 20  $\mu$ g of cell lysate input (input) are shown. (D) Nuclear and cytoplasmic extracts were prepared from MEER cells after transfection with pCMV (empty vector) or pCMV-mouse CD200. The expression level of each protein was determined by western blot analysis. (E) Total protein extracted from MEER cell lines ( $1 \times 10^6$  cells) was used for western blot analysis. c-MYC and S100A4 were evaluated as the target genes of  $\beta$ -catenin. (F) NF $\kappa$ B transcriptional activity was measured in MEER and MEER/CD200<sup>High</sup> cells 24 h post transfection with the NF $\kappa$ B luciferase reporter vector and the CD200 overexpression vector for 24 h. (G) Total protein from MEER/CD200<sup>High</sup> cells was extracted for immunoblot analysis of the key NF $\kappa$ B pathway proteins. (H) MEER/CD200<sup>High</sup> cells ( $2 \times 10^5$ ) were treated with 20 pmol of CD200 siRNA (top panel) or purified sCD200R1 as described in (B) (bottom panel). Cells were lysed with RIPA buffer 24 h post transfection. Extracted proteins (30  $\mu$ g) were resolved by western blot analysis with the corresponding antibodies. (I) NF $\kappa$ B transcriptional activity was measured in MEER and MEER/CD200<sup>High</sup> cells treated with CD200 siRNA or Ad5sCD200R1. (J) The localization of phosphorylated p65 was monitored by confocal microscopy. Phosphorylated p65 was labeled with a rhodamine-conjugated antibody, and the cytoskeleton was stained with Alexa Fluor 488-conjugated phalloidin.

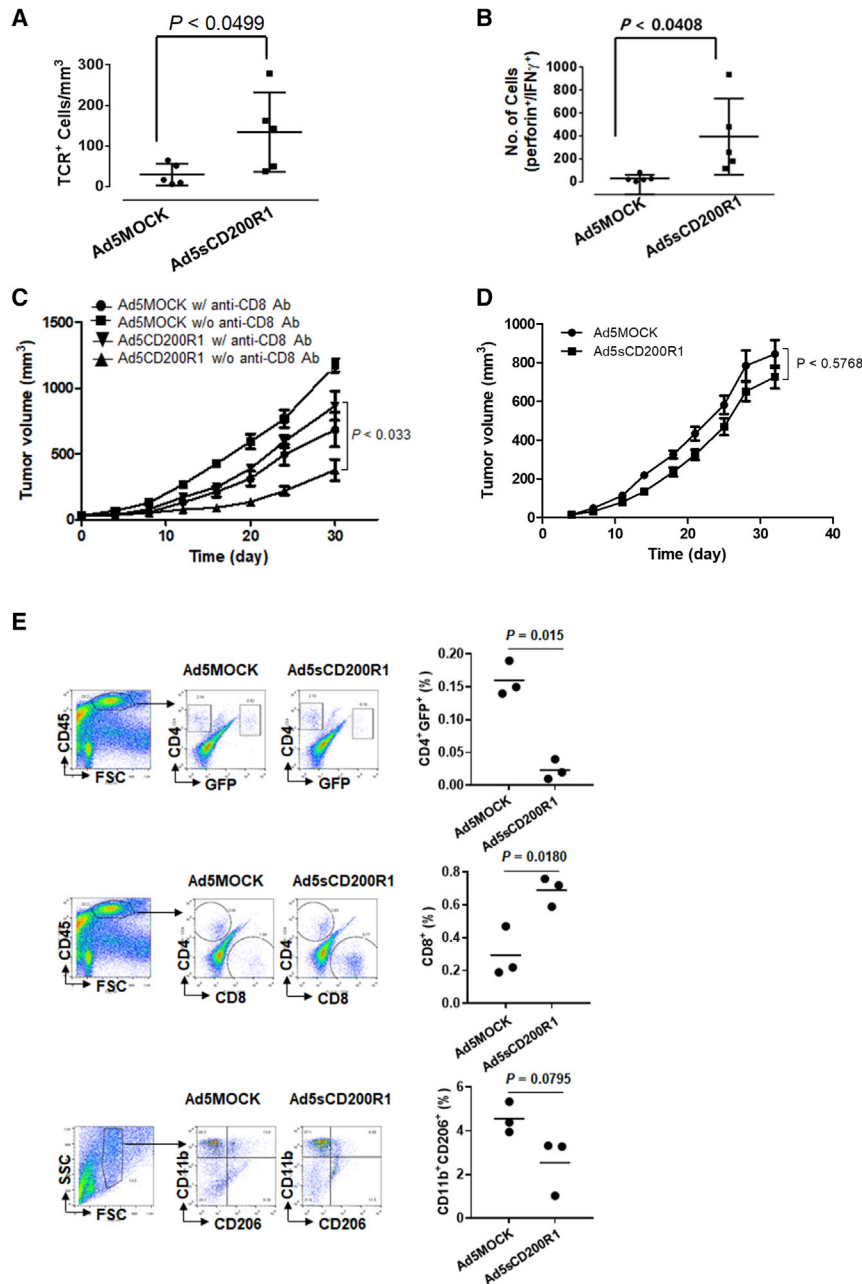


**Figure 6. Effects on CD8<sup>+</sup> T cells and Treg cells in tumor upon CD200 blockade**

(A) Subcutaneous MEER/CD200<sup>High</sup> tumors in C57BL/6 mice were injected with  $5 \times 10^8$  PFUs of Ad5MOCK and Ad5sCD200R1. The tumors were harvested at the time of euthanization. The number of T cells was calculated based on the number of CD45<sup>+</sup>TCR<sup>+</sup> cells as determined by flow cytometry. The calculated number of CD45<sup>+</sup>TCR<sup>+</sup> cells was divided by the tumor size in the host. (B) Tumors obtained from the same mouse model described in (A) were analyzed by flow cytometry using anti-Perforin and anti-IFN- $\gamma$  antibodies right after gating CD45<sup>+</sup> cells. (C) Subcutaneous MEER/CD200<sup>High</sup> tumors in C57BL/6 mice were injected with  $5 \times 10^8$  PFUs of Ad5MOCK or Ad5sCD200R1. One day before virus treatment and every 5 days after treatment, mice were injected intraperitoneally with the anti-CD8 antibody (clone 2.43, 500  $\mu$ g) to deplete CD8<sup>+</sup> T cells. (D) Subcutaneous MEER/CD200<sup>High</sup> tumors in BALB/c-nude mice were injected with  $5 \times 10^8$  PFUs of Ad5MOCK or Ad5sCD200R1. Tumor growth was monitored and plotted at the indicated time points. (E) C57BL/6-Tg (Foxp3-GFP)<sup>90P</sup>Kraj/J transgenic mice were subcutaneously implanted with MEER/CD200<sup>High</sup> cells and palpable tumors were injected twice with  $5 \times 10^8$  PFUs of Ad5MOCK or Ad5sCD200R1 on day 3 and on day 7. Tumors were harvested from mice on day 10. CD45<sup>+</sup>GFP<sup>+</sup>CD4<sup>+</sup> regulatory T cells were detected by flow cytometry. p values were determined by two-tailed unpaired t tests.

gated by neutralizing sCD200R1-Ig. Interestingly, sCD200R1-Ig treatment polarized even M2-like macrophages to M1-like macrophages, although weakly. Indeed, the tumor suppression mediated by Ad5sCD200R1 in cultures with MEER/CD200<sup>High</sup> cells could be mainly due to the inhibition of CD200-driven M2-like polarization and the induction of M1-like macrophage polarization in the TIME. In this study, we showed that the promotive effect of CD200 on protumor M2-like polarization is mediated through the  $\beta$ -catenin/S100a4-RAGE/NF $\kappa$ B/M-CSF axis in tumor cells. Binding of CD200 to  $\beta$ -catenin was confirmed. This finding indicates that CD200 is not only a binding partner of CD200R1 but also an immune modulator independent of CD200R1. Indeed, not only TCR<sup>+</sup>

cells and perforin<sup>+</sup>/IFN- $\gamma$ <sup>+</sup> effector T cells but also CD4<sup>+</sup>CD25<sup>+</sup> regulatory T cells might be diverse critical players.

Taken together, our findings indicated that in solid cancers such as HNSCC, the myeloid immune checkpoint molecule CD200 exclusively induced M2-like polarization in the TIME by binding  $\beta$ -catenin and stimulating the S100A4-RAGE/NF- $\kappa$ B/M-CSF axis in tumor cells. In parallel, PD-L1 expression was so dramatically induced by IFN- $\gamma$  in a CD200-rich environment *in vitro* that combined targeting of PD1

the pattern observed in TCGA data. Furthermore, the interspecies homology of CD200 between humans and mice in the DNA (81.7%) and protein (77.6%) sequences<sup>25</sup> could imply similarity between the mouse model and clinical conditions. We initially hypothesized that CD200 induces tumor growth by driving M2-like polarization through increased expression of M-CSF. In line with our prediction and a previous report,<sup>26</sup> BMCs and M1-like macrophages (F4/80<sup>+</sup>CD206<sup>-</sup>) co-cultured with MEER/CD200<sup>High</sup> cells were polarized into M2-like macrophages (F4/80<sup>+</sup>CD206<sup>+</sup>). Furthermore, this effect was abro-

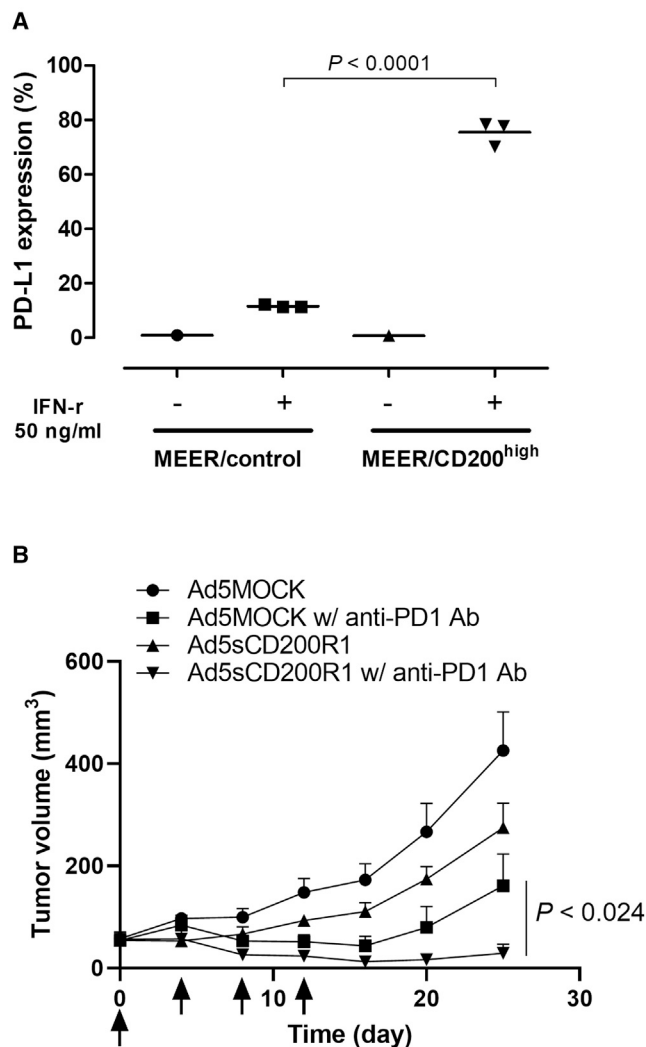


**Figure 7. Anti-tumor effects by targeting both CD200 and PD1**

(A) (Left panel) MEER/control and MEER/CD200<sup>High</sup> cells ( $2 \times 10^4$ ) were seeded in 6-well plates. PD-L1 expression was measured by flow cytometry 3 days after treatment with 50 ng/mL IFN- $\gamma$ . (B) C57BL/6 mice were subcutaneously injected with  $1 \times 10^6$  of MEER/CD200<sup>High</sup> cells. Each adenovirus of Ad5MOCK or Ad5sCD200R1 of  $5 \times 10^8$  PFUs was intratumorally injected 3 times at 4-day intervals. For combination therapy, anti-mouse PD-1 antibody of 200  $\mu$ g was intraperitoneally injected 4 times at 4-day intervals. Arrows indicate the times of adenovirus and antibody injection. *p* values were determined by two-tailed paired *t* tests.

and CD200 by local injection of Ad5sCD200R1 adenovirus potentiated the antitumor effect. Extrapolation from replication-deficient adenoviruses expressing sCD200R1-Ig suggests that the effects of replication-competent adenoviruses such as ONYX-015<sup>27</sup> could be potentiated by simultaneous expression of sCD200R1-Ig in clinical settings.

## MATERIALS AND METHODS

### Cells and mice

Immortalized mouse tonsillar epithelium with E6, E7, and Ras (MEER) cells were generated and used to establish a murine model

for HPV16+ HNSCC.<sup>28</sup> MEER/CD200<sup>High</sup> cells were generated by stably transfecting cells with the pUNO1.mouseCD200 plasmid,<sup>12</sup> which is a subclone of clone #13 used in our previous publication (InvivoGen, San Diego, CA, USA).<sup>13</sup> MEER/control, MEER/CD200<sup>High</sup>, HEK293, and HEK293T cells were cultured in DMEM containing 10% fetal bovine serum (FBS; GE Healthcare, Chicago, IL, USA) and 1% penicillin/streptomycin (Thermo Fisher Scientific, Waltham, MA, USA). Six- to eight-week-old female BALB/c-nude and C57BL/6 mice were purchased from OrientBio (Sungnam, Korea). All animal experiments were performed in accordance with the Guidelines for the Care and Use of Laboratory Animals of the National Cancer Center, Goyang, Korea.

### Analysis of TCGA data

Total RNA of MEER/CD200<sup>High</sup> cells was extracted using an RNeasy Mini Kit (QIAGEN, Hilden, Germany). The normalized read counts from MEER cell mRNA expression data were obtained using the Illumina NextSeq 500 platform (Illumina, San Diego, CA, USA). Fold change values were calculated for “immune response” category genes that were differentially expressed in CD200<sup>High</sup> versus control cells (fold change > 1.5, *p* < 0.05). TCGA mRNAseq data for 522 patients with HNSCC were downloaded from cBioPortal.<sup>29,30</sup> We then compared the genes with significantly increased expression levels after CD200 overexpression between the datasets (MEER CD200<sup>High</sup> cells versus TCGA data). A *p* value < 0.05 and a fold change > 1.5 were considered to indicate a statistically significant difference in expression.

### Coculture of bone-marrow-derived macrophages and MEER cells

BMCs were harvested from the femurs and tibias of female C57BL/6 mice, dispersed into RPMI 1640 medium, and cultured in RPMI 1640 medium containing 10% (w/v) FBS, 100 U/mL penicillin/streptomycin (Invitrogen, Carlsbad, CA, USA), and either GM-CSF or M-CSF. Recombinant GM-CSF or M-CSF (10 ng/mL) was used for differentiation into M1 or M2 macrophages. The medium was changed every other day for 7 days. For polarization into the M1-like or M2-like phenotype, M1-like or M2-like macrophages were stimulated with 50 ng/mL IFN- $\gamma$  or 10 ng/mL IL-4. MEER/control or MEER/CD200<sup>High</sup> cells ( $2 \times 10^4$ ) were seeded and cocultured with BMCs ( $2 \times 10^6$ ) for 5 days. Fully polarized M1 or M2 macrophages ( $2 \times 10^5$  cells) were cocultured with  $2 \times 10^4$  MEER/control or MEER/CD200<sup>High</sup> cells for 3 days. These cocultures were exposed to 4  $\mu$ g of purified sCD200R1-Ig for 3 days to neutralize CD200.

### Adenovirus construction

Ad5sCD200R1 was constructed with AdenoZAP<sup>TM</sup> 1.2 kits for truncation of E1 and E3 (OD260, Boise, ID, USA). The construct containing the extracellular domain of mouse CD200 receptor 1 fused with mouse Fc1 was called sCD200R1-Ig. To generate sCD200R1-Ig, the extracellular domain of mouse CD200R1 (OriGene, Montgomery County, MD, USA) was amplified by PCR using two primers: 5'-GAA TTC GCC ACC ATG TTT TGC TTT TGG-3' and 5'-CAA TGG CTC CTC CTC CTC GTA ATG ATT GGT T-3'. The amplified

product was inserted into the *EcoRI/NcoI* site in pFUSE-mIgG2A.Fc1, which contains the EF1 $\alpha$  promoter, Fc1 of mIgG2A, and the SV40 poly A sequence (InvivoGen, San Diego, CA, USA), resulting in the fusion of sCD200R1 with Fc1 of IgG2a. Then, EF1 $\alpha$ .sCD200R1 was subcloned into the *NotI/EcoRV* site in a viral shuttle vector, pZAP1.1 (OD260, Boise, ID, USA), to generate pZAP1.1.EF1 $\alpha$ .sCD200R1.Fc1. To construct Ad5sCD200R1, pZAP1.1.EF1 $\alpha$ .sCD200R1.Fc1 was digested with *DraIII/PacI/ClaI*, ligated with RightZAP1.2 (OD260, Boise, ID, USA), and transfected into HEK293 cells. The control adenovirus Ad5MOCK was prepared and used as previously described.

#### Western blot analysis, flow cytometry, and immunohistochemistry

Cells were lysed in radioimmunoprecipitation assay (RIPA) buffer containing protease inhibitors (Sigma-Aldrich, St. Louis, MO, USA). Antibody-antigen complexes on PVDF membranes were quantified using ImageQuant software (Molecular Dynamics, San Diego, CA, USA). Antibodies specific for the following proteins were used: phosphorylated p65 (Cell Signaling Technology, Danvers, MA, USA); phosphorylated I $\kappa$ B $\alpha$  (Ser32/36) (Cell Signaling Technology); phosphorylated IKK $\alpha$ / $\beta$  (Ser176/180) (Cell Signaling Technology); CD200 (R&D Systems, Minneapolis, MN, USA); CD200R1 (R&D Systems, Minneapolis, MN, USA), S100A4 (R&D Systems); c-MYC (Cell Signaling Technology); RAGE (R&D Systems);  $\beta$ -catenin (Merck, Palo Alto, CA, USA); M-CSF (R&D Systems); and  $\beta$ -actin (Santa Cruz, TX, USA). For flow cytometric analysis, all cells ( $1 \times 10^7$ ) or dissociated tumors were incubated for 15 minutes in the dark with an anti-mouse CD16/CD32 antibody (BD Biosciences, San Jose, CA, USA). MEER/CD200<sup>High</sup> cells, M1/M2-like macrophages, regulatory T cells, CD45<sup>+</sup>CD4<sup>+</sup> T cells, and CD45<sup>+</sup>CD8<sup>+</sup> T cells were detected with PE-conjugated anti-CD200 (BD Biosciences), PE-conjugated anti-F4/80, FITC-conjugated anti-CD206, FITC-conjugated anti-TCR V $\alpha$ 2, APC-conjugated anti-IFN- $\gamma$ , PE-conjugated anti-Perforin, PE-conjugated anti-CD45, FITC-conjugated anti-CD4, and FITC-conjugated anti-CD8 (BioLegend, San Diego, CA, USA) antibodies. All cells were washed with FACS buffer (0.2% BSA, 0.1% sodium azide, and 2 mM EDTA). Data were acquired with a FACSVerser flow cytometer (BD Biosciences) and analyzed with FlowJo (Tree Star, OR, USA). For immunofluorescence staining of phosphorylated p65,  $1 \times 10^4$  cells were seeded onto cover glasses in 12-well plates and blocked with PBS containing 3% BSA. Then, a rabbit polyclonal antibody against phospho-p65 (Cell Signaling Technologies) was incubated with cells overnight at 4°C and rinsed with PBS containing 0.05% tween 20. Cells were incubated with rhodamine-conjugated anti-rabbit antibodies and a phalloidin-conjugated anti-F-actin compound (Life Technologies, Grand Island, NY, USA) for 2 h at room temperature. Fluorescence images were acquired using a confocal microscope.

#### Immunoprecipitation assays

Cell lysates (obtained after transfection of the pCMV-3AG-3a-EV or pCMV-3AG-3a-CD200 construct) containing 1 mg of protein were precleared by incubation with 40  $\mu$ L of protein-A/G linked agarose

beads (Santa Cruz) for 1 h at 4°C. After the beads were pelleted by centrifugation, the supernatant was incubated with 40  $\mu$ L of anti-FLAG M2 affinity gel (Sigma-Aldrich) overnight at 4°C. After incubation, the beads were washed 3 times in RIPA buffer before being dissolved in SDS-PAGE loading buffer. Then, western blot analysis was performed. For fractionation of cellular extracts, MEER cells were transfected with the pCMV vector or pCMV-mouseCD200 vector. Nuclear and cytoplasmic extracts were prepared as described previously.<sup>31</sup>

#### Transient transfection and PCR analysis

Cells were seeded at  $2 \times 10^5$  cells/well and transiently transfected with a small interfering RNA (siRNA) targeting mouse CD200 or a scrambled siRNA (Origene Technologies, Rockville, MD, USA). For each transfection, 20 pmol of siRNA in 500  $\mu$ L of serum-free Opti-MEM mixed with 7  $\mu$ L of Lipofectamine RNAiMAX (Invitrogen) was used. Total RNA was extracted from each cell line using TRIzol (Invitrogen) according to the manufacturer's protocols. cDNA synthesis was performed in a solution with a total volume of 10  $\mu$ L using QIAGEN Omniscript RT kits (QIAGEN). PCR was performed using primers specific for *mouse CD200* (5'-AAA CAT CCC AGG AAC CCT TG-3' and 5'-TGT CTT TGT AGG CAG GCT GG-3'), *M-CSF* (5'-CAG CTG CTT CAC CAA GGA CT-3' and 5'-TCA TGG AAA GTT CGG ACA CA-3'), and *GAPDH* (5'-CCA CCA CCC TGT TGT AG-3' and 5'-CCC ACT CTT CCA CCT TCG AT-3') with the following thermal cycling conditions: preheating for 10 minutes at 95°C; 30 cycles of amplification for 30 s at 95°C, 30 s at 60°C, and 30 s at 72°C; and final extension for 10 minutes at 72°C. All measurements were performed in triplicate.

#### Animal experiments

Female C57BL/6 mice and C57BL/6-Tg (Foxp3-GFP)90Pkrj/J (The Jackson Laboratory, Bar Harbor, ME, USA) of 6 to 8 weeks old were inoculated subcutaneously with  $1 \times 10^6$  MEER/CD200<sup>High</sup> or MEER/control cells. When tumors were palpable (approximately day 10 to 13),  $5 \times 10^8$  PFUs of adenovirus were injected intratumorally 3 times at 4-day intervals. Tumors were harvested from the mice after euthanasia, and tumor tissues were then dissociated using a tumor dissociation kit (Miltenyi Biotec, Bergisch Gladbach, Germany). For macrophage depletion studies, 1.4 mg of a clodronate liposome formulation, Clophosome (FormuMax Scientific, Sunnyvale, CA, USA), was intraperitoneally injected before the first injection of adenovirus and was then administered (0.7 mg) every 4 days for a total of three treatments. For CD8<sup>+</sup> T cell depletion studies, an anti-CD8 depletion antibody (clone 2.43) was injected intraperitoneally one day before virus injection and was then administered (500  $\mu$ g) 6 times at 5-day intervals. For combination therapy of Ad5CD200R1 with anti-PD1 antibodies, anti-mouse PD-1 (Bioxcell, Lebanon, NH, USA) was injected intraperitoneally (400  $\mu$ g) 4 times at 4-day intervals. Tumor volumes were determined using the following formula: tumor volume ( $\text{mm}^3$ ) = length  $\times$  width<sup>2</sup>  $\times$  0.5236.

#### Statistical analysis

Comparisons between two groups were made using two-tailed paired t tests or unpaired t tests. Two-tailed p values <0.05 were considered

significant. STATA/SE version 10.1 software (StataCorp LP, College Station, TX, USA) was used for analyses.

## SUPPLEMENTAL INFORMATION

Supplemental information can be found online at <https://doi.org/10.1016/j.omto.2021.09.001>.

## ACKNOWLEDGMENTS

This study was supported by National Cancer Center Grant, Korea (NCC-1910011). This study was reviewed and approved by the Institutional Animal Care and Use Committee (IACUC) of National Cancer Center Research Institute (NCCRI). NCCRI is an Association for Assessment and Accreditation of Laboratory Animal Care International (AAALAC International) accredited facility and abide by the Institute of Laboratory Animal Resources (ILAR) guide.

## AUTHOR CONTRIBUTIONS

A.-R.G., J.-M.J., H.-G.K., S.-J.K., J.-K.K., and S.-P.S. prepared Figures 1, 2, 3, 4, 5, 6, and 7 by performing most of experiments reported in this manuscript. Y.-S.B. and E.-J.P. put forward idea of the paper. S.-J.L., Y.-S.J., and K.C. wrote the main manuscript text. All authors reviewed and approved the final manuscript.

## DECLARATION OF INTERESTS

The authors declare no competing interests

## REFERENCES

- Leach, D.R., Krummel, M.F., and Allison, J.P. (1996). Enhancement of antitumor immunity by CTLA-4 blockade. *Science* 271, 1734–1736.
- Hodi, F.S., Mihm, M.C., Soffier, R.J., Haluska, F.G., Butler, M., Seiden, M.V., Davis, T., Henry-Spires, R., MacRae, S., Willman, A., et al. (2003). Biologic activity of cytotoxic T lymphocyte-associated antigen 4 antibody blockade in previously vaccinated metastatic melanoma and ovarian carcinoma patients. *Proc. Natl. Acad. Sci. USA* 100, 4712–4717.
- Dong, H., Strome, S.E., Salomao, D.R., Tamura, H., Hirano, F., Flies, D.B., Roche, P.C., Lu, J., Zhu, G., Tamada, K., et al. (2002). Tumor-associated B7-H1 promotes T-cell apoptosis: a potential mechanism of immune evasion. *Nat. Med.* 8, 793–800.
- Brahmer, J.R., Drake, C.G., Wollner, I., Powderly, J.D., Picus, J., Sharfman, W.H., Stankevich, E., Pons, A., Salay, T.M., McMiller, T.L., et al. (2010). Phase I study of single-agent anti-programmed death-1 (MDX-1106) in refractory solid tumors: safety, clinical activity, pharmacodynamics, and immunologic correlates. *J. Clin. Oncol.* 28, 3167–3175.
- Erin, N., Podnos, A., Tanriover, G., Duymuş, Ö., Cote, E., Khatri, I., and Gorczynski, R.M. (2015). Bidirectional effect of CD200 on breast cancer development and metastasis, with ultimate outcome determined by tumor aggressiveness and a cancer-induced inflammatory response. *Oncogene* 34, 3860–3870.
- Kawasaki, B.T., and Farrar, W.L. (2008). Cancer stem cells, CD200 and immunoevasion. *Trends Immunol.* 29, 464–468.
- Clark, D.A., Arredondo, J.L., and Dhesy-Thind, S. (2015). The CD200 tolerance-signaling molecule and its receptor, CD200R1, are expressed in human placental villus trophoblast and in peri-implant decidua by 5 weeks' gestation. *J. Reprod. Immunol.* 112, 20–23.
- Coles, S.J., Gilmour, M.N., Reid, R., Knapper, S., Burnett, A.K., Man, S., Tonks, A., and Darley, R.L. (2015). The immunosuppressive ligands PD-L1 and CD200 are linked in AML T-cell immunosuppression: identification of a new immunotherapeutic synapse. *Leukemia* 29, 1952–1954.
- Vaine, C.A., and Soberman, R.J. (2014). The CD200-CD200R1 inhibitory signaling pathway: immune regulation and host-pathogen interactions. *Adv. Immunol.* 121, 191–211.
- Choueiry, F., Torok, M., Shakya, R., Agrawal, K., Deems, A., Benner, B., Hinton, A., Shaffer, J., Blaser, B.W., Noonan, A.M., et al. (2020). CD200 promotes immunosuppression in the pancreatic tumor microenvironment. *J. Immunother. Cancer* 8, e000189.
- Kretz-Rommel, A., Qin, F., Dakappagari, N., Cofield, R., Faas, S.J., and Bowdish, K.S. (2008). Blockade of CD200 in the presence or absence of antibody effector function: implications for anti-CD200 therapy. *J. Immunol.* 180, 699–705.
- Shin, S.P., Seo, H.H., Shin, J.H., Park, H.B., Lim, D.P., Eom, H.S., Bae, Y.S., Kim, I.H., Choi, K., and Lee, S.J. (2013). Adenovirus expressing both thymidine kinase and soluble PD1 enhances antitumor immunity by strengthening CD8 T-cell response. *Mol. Ther.* 21, 688–695.
- Shin, S.P., Goh, A.R., Kang, H.G., Kim, S.J., Kim, J.K., Kim, K.T., Lee, J.H., Bae, Y.S., Jung, Y.S., and Lee, S.J. (2019). CD200 Induces Epithelial-to-Mesenchymal Transition in Head and Neck Squamous Cell Carcinoma via  $\beta$ -Catenin-Mediated Nuclear Translocation. *Cancers (Basel)* 11, E1583.
- Kretz-Rommel, A., Qin, F., Dakappagari, N., Ravey, E.P., McWhirter, J., Oltean, D., Frederickson, S., Maruyama, T., Wild, M.A., Nolan, M.J., et al. (2007). CD200 expression on tumor cells suppresses antitumor immunity: new approaches to cancer immunotherapy. *J. Immunol.* 178, 5595–5605.
- Ring, E.K., Markert, J.M., Gillespie, G.Y., and Friedman, G.K. (2017). Checkpoint Proteins in Pediatric Brain and Extracranial Solid Tumors: Opportunities for Immunotherapy. *Clin. Cancer Res.* 23, 342–350.
- Binns, D., Dimmer, E., Huntley, R., Barrell, D., O'Donovan, C., and Apweiler, R. (2009). QuickGO: a web-based tool for Gene Ontology searching. *Bioinformatics* 25, 3045–3046.
- Hamilton, T.A., Zhao, C., Pavicic, P.G., Jr., and Datta, S. (2014). Myeloid colony-stimulating factors as regulators of macrophage polarization. *Front. Immunol.* 5, 554.
- Trus, E., Basta, S., and Gee, K. (2020). Who's in charge here? Macrophage colony stimulating factor and granulocyte macrophage colony stimulating factor: Competing factors in macrophage polarization. *Cytokine* 127, 154939.
- Hou, S., Tian, Q., Qi, D., Sun, K., Yuan, Q., Wang, Z., Qin, Z., Wu, Z., Chen, Z., and Zhang, J. (2018). S100A4 promotes lung tumor development through  $\beta$ -catenin pathway-mediated autophagy inhibition. *Cell Death Dis.* 9, 277.
- Brach, M.A., Henschler, R., Mertelsmann, R.H., and Herrmann, F. (1991). Regulation of M-CSF expression by M-CSF: role of protein kinase C and transcription factor NF kappa B. *Pathobiology* 59, 284–288.
- Glass, C.K., and Natoli, G. (2016). Molecular control of activation and priming in macrophages. *Nat. Immunol.* 17, 26–33.
- Gaiser, M.R., Weis, C.A., Gaiser, T., Jiang, H., Buder-Bakhaya, K., Herpel, E., Warth, A., Xiao, Y., Miao, L., and Brownell, I. (2018). Merkel cell carcinoma expresses the immunoregulatory ligand CD200 and induces immunosuppressive macrophages and regulatory T cells. *OncoImmunology* 7, e1426517.
- Dias, J.D., Guse, K., Nokisalmi, P., Eriksson, M., Chen, D.T., Diaconu, I., Tenhunen, M., Liikanen, I., Grénman, R., Savontaus, M., et al. (2010). Multimodal approach using oncolytic adenovirus, cetuximab, chemotherapy and radiotherapy in HNSCC low passage tumour cell cultures. *Eur. J. Cancer* 46, 625–635.
- Li, D., Duan, L., Freimuth, P., and O'Malley, B.W., Jr. (1999). Variability of adenovirus receptor density influences gene transfer efficiency and therapeutic response in head and neck cancer. *Clin. Cancer Res.* 5, 4175–4181.
- Walker, D.G., and Lue, L.F. (2013). Understanding the neurobiology of CD200 and the CD200 receptor: a therapeutic target for controlling inflammation in human brains? *Future Neurol.* 8.
- Mantovani, A., Sozzani, S., Locati, M., Allavena, P., and Sica, A. (2002). Macrophage polarization: tumor-associated macrophages as a paradigm for polarized M2 mononuclear phagocytes. *Trends Immunol.* 23, 549–555.
- Nemunaitis, J., Ganly, I., Khuri, F., Arseneau, J., Kuhn, J., McCarty, T., Landers, S., Maples, P., Romel, L., Randlev, B., et al. (2000). Selective replication and oncolysis in p53 mutant tumors with ONYX-015, an E1B-55kD gene-deleted adenovirus, in

- patients with advanced head and neck cancer: a phase II trial. *Cancer Res.* 60, 6359–6366.
28. Jung, Y.S., Vermeer, P.D., Vermeer, D.W., Lee, S.J., Goh, A.R., Ahn, H.J., and Lee, J.H. (2015). CD200: association with cancer stem cell features and response to chemoradiation in head and neck squamous cell carcinoma. *Head Neck* 37, 327–335.
29. Cerami, E., Gao, J., Dogrusoz, U., Gross, B.E., Sumer, S.O., Aksoy, B.A., Jacobsen, A., Byrne, C.J., Heuer, M.L., and Larsson, E. (2012). The cBioPortal: an open platform for exploring multidimensional cancer genomics data (AACR).
30. Gao, J., Aksoy, B.A., Dogrusoz, U., Dresdner, G., Gross, B., Sumer, S.O., Sun, Y., Jacobsen, A., Sinha, R., Larsson, E., et al. (2013). Integrative analysis of complex cancer genomics and clinical profiles using the cBioPortal. *Sci. Signal.* 6, p11.
31. Kim, S.J., Lee, H.W., Gu Kang, H., La, S.H., Choi, I.J., Ro, J.Y., Bresalier, R.S., Song, J., and Chun, K.H. (2014). Ablation of galectin-3 induces p27(KIP1)-dependent premature senescence without oncogenic stress. *Cell Death Differ.* 21, 1769–1779.